BEARING CAPACITY OF A SINGLE PILE IN SATURATED AND DRAINED CLAY

NOSILNOST POSAMIČNEGA PILOTA V ZASIČENI GLINI PRI DRENIRANIH POGOJIH

Yu Song
China University of Petroleum,
State Key Laboratory of Marine Oil and Gas Drilling and Completion
Beijing, China
E-mail: songyu_cup@163.com

Jin Yang *(corresponding author)*
China University of Petroleum,
State Key Laboratory of Marine Oil and Gas Drilling and Completion
Beijing, China
E-mail: cyjin1018@vip.sina.com

Hua Xiang
Gubkin Russian State University of Oil and Gas,
Department of development of offshore oil and gas fields
Moscow, Russia
E-mail: xiang.h@gubkin.ru

Bo Zhou
CNPC Engineering Technology R&D Company Limited,
Department of Oil and Gas Drilling and Completion
Beijing, China
E-mail: zhoubodr@cnpc.com.cn

DOI https://doi.org/10.18690/actageotechslov.16.1.70-78.2019

Keywords

laterally loaded pile; bend moment; force-displacement (p-y) curve; soil resistance

Ključne besede

bočno obtežen pilot; upogibni moment; krivulja sila--premik (p-y); odpornost tal

Abstract

In this study the pile-soil interaction behavior of single, long, laterally loaded, embedded piles was investigated in both saturated and drained clay. The piles were hollow steel pipes with a diameter of 114 mm, a thickness of 2.5 mm, and a length-to-diameter ratio of 35. The piles were installed in inhomogeneous, saturated clay and laterally loaded to test their mechanical behaviors in saturated and drained soil. The soil-pile interaction force-displacement relationships (p-y curves) were calculated from the soil reaction and combined with the directly measured lateral displacement. The results indicate that the lateral load--bearing capacity of the pile in drained clay is up to 27% greater than the initial value. Furthermore, the ultimate soil resistance in both types of clay increases linearly with depth. There is a large difference between drained clay and unsaturated loose clay. The soil resistance in drained clay is nearly two times larger than that in unsaturated clay. This study also compares and analyzes the difference between the measured p-y curves and the back-calculated values.

Izvleček

V predstavljeni študiji je bilo preučevano interakcijsko vedenje posamičnih, dolgih, bočno obteženih pilotov v zasičenih in dreniranih glinah. Piloti so bili izdelani iz votlih jeklenih cevi premera 114 mm, debeline 2,5 mm, razmerje med dolžino in premerom je bilo enako 35. Piloti so bili vgrajeni v nehomogenih zasičenih glinah in bočno obteženi, da bi preverili njihovo mehansko obnašanje v zasičeni in drenirani zemljini. Interakcijo zemljina-pilot v obliki relacije sila-pomik (p-y krivulje) smo izračunali iz reakcije zemljine in neposredno izmerjenim bočnim premikom. Rezultati kažejo, da je bočna nosilnost pilota v drenirani glini do 27% večja od njene začetne vrednosti. Poleg tega se mejna odpornost tal pri obeh vrstah gline linearno povečuje z globino. Obstaja velika razlika med drenirano glino in nezasičeno mehko glino. Odpornost tal v drenirani glini je skoraj dvakrat večja od njene vrednosti v nezasičeni glini. Študija vsebuje tudi primerjavo in analizo razlike med izmerjenimi krivuljami p-y in vrednostmi dobljenimi s povratnimi analizami.

1 INTRODUCTION

The stability of piles that are used to support oceanographic engineering, oil and gas wellheads, buildings, bridges, transmission lines, and highway structures is commonly governed by lateral loads [1]. In areas with high rainfall and numerous beaches and rivers, the soil around a pile will undergo a process of natural drainage from the saturated to the unsaturated state; this can lead to changes in the lateral bearing capacity of the pile.

The issue of soil modeling is also important in the perspective of ensuring sustainable production from the productive formations [2-3].

Many studies have investigated the pile-soil interface and lateral bearing capacity in saturated and unsaturated soil. However, a comparative study of soil resistance in saturated and drained clay has not been conducted. Studies have also analyzed the large horizontal deformation of piles in detail, in order to clarify the internal relations between the deformation and the internal forces and the lateral soil resistance [4-5]. These characteristics have important scientific and engineering significance for the development of a clay strata construction.

The response analysis of the lateral pile deflection and the lateral soil resistance is important for designing laterally loaded piles. Numerous studies have applied elastic and elastoplastic analytical methods to transverse piles [6-8]. Popular elastic analysis methods include the foundation-beam method, the finite-element method, and the boundary-element method. However, it is difficult to use these methods to accurately predict the actual behavior of a pile foundation when laterally loaded piles are deformed significantly [9-10].

The elastoplastic analysis model is more reasonable when the pile foundation has a large horizontal deformation. The engineering community considers the p-y curve method the most effective analytical method for a pile foundation with a large horizontal displacement [11]. The p-y curve is a comprehensive index that reflects the resistance of the surrounding soil to the pile body. It is influenced by many factors, such as the pile diameter, the pile foundation stiffness, the cross-sectional shape, the size effect, and the pile head restraint condition [12]. Matlock established the p-y curve of saturated soft clay and Reese established that of saturated sandy soil through experimental methods [5, 13]. The p-y curve method has subsequently been adopted and promoted by the American Petroleum Institute [14]. However, some experimental studies have noted a certain deviation when using the soil shear strength and pile bending moment to derive the soil resistance [5, 7, 15].

In recent years, studies have actively investigated pile-soil contact in unsaturated soils. Many studies have focused on finding differences between unsaturated and saturated soils and on establishing and modifying the mathematical functions of soil resistance [16-19]. However, the physical properties of saturated and unsaturated clays generally differ significantly. Experimental measurements normally use the direct shear test and the particle size of loose dry clay in saturated clay [20-21]. In addition, studies have measured the pile bending moment to estimate the soil resistance instead of using direct measurements. To the best of our knowledge, no study has investigated the soil-pile contact effect in the saturated clay drainage process.

In this study, advanced sensors were used to measure directly the pile bending moment, the pile body displacement, and the soil resistance. Subsequently, a reasonable p-y curve was derived for responses to changes in the soil properties.

2 METHOD

2.1 Experimental Materials

This experiment used clay soil samples obtained at China Bohai Beach. The saturated soil samples were prepared in the soil pool by using sorted soil that was collected on site. The laboratory measurement results of the saturated soil samples are based on the Unified Soil Classification System [22]. Figure 1 shows the particle size distribution and the composition of the slightly sandy silty clay soil samples (uniform coefficient, C_u 8.4). The maximum and minimum unit weights of the well-graded sand in an oven-dried condition were 2.05 and 1.61 kN/m^3, respectively.

The pile used in the test was a hollow circular steel tube with a measured elastic modulus of 206 GPa, an outside diameter of 114 mm, and a thickness of 2.5 mm. The yield bending moment of the pile body ([M]) obtained by the deflection measurement method was 7260 kN·m. Boominathan and Ayothiraman [23] divided the embedment length of the pile according to its mechanical behavior. Studies have already suggested that a pile with a length-to-diameter ratio (L/D) < 20 appears as a short stiff pile, a pile with L/D = 20 appears as an intermediate pile, and a pile with L/D > 25 appears as a long flexible pile. The experiment used a pile with a depth of 3990 mm and a L/D of 35. Table 1 shows the basic parameters of the pile and the relative stiffness of the soil. The load application point of the pile was 100 mm above the mud surface.

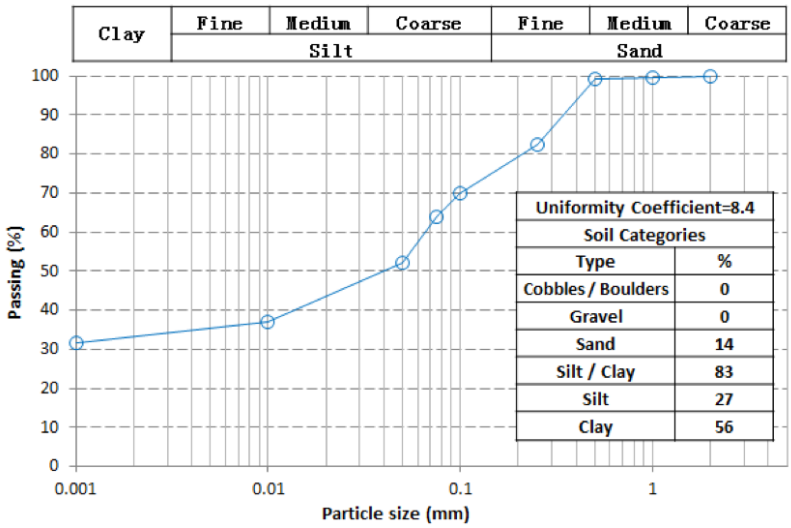

Figure 1. Properties of the slightly sandy silty clay soil used in the experiment.

Table 1. Parameters of the pile and the relative stiffness of the soil.

Outside diameter (mm)	Wall thickness (mm)	Stiffness (EI) ($\times 10^9$N/mm^2)	Embedment length (mm)	Pile length (mm)	Length-to-diameter ratio	Description
114	2.5	309	3990	4090	35	Long flexible

2.2 Pile-Soil Interaction Experimental Facility

The pile-soil interaction (PSI) facility comprised a testing soil pool, a lateral loading control system, and various sensor and data-acquisition components. The testing soil pool had dimensions of 6.0 × 3.0 × 5.0 m^3 and three drains installed in its bottom. The soil thickness was 4.8 m, and the length and width were more than 10 times the outside diameter of the pile. The measurement results were not affected by the boundary effect [24]. A lateral loading control system applied lateral loads to the pile head, and it controlled and recorded the output load value. The loads applied to the pile head were varied from 980 to 9800 N in increments of 980 N. For each load increment, the load was kept constant until the lateral displacement of the pile stabilized.

The PSI facility includes thin resistance strain gauges, a customized inclinometer sensor, and soil-pressure sensors. The resistance strain gauges, each having

Figure 2. Pile-soil interaction experimental facility.

a length of 6 mm and a resistance of 120 Ω, were installed below the mud surface on the tension side of the pile at 228-mm intervals (0, 228, 456, 684, 912, 1140, 1368, 1596, 1824, 2052, 2280, 2508, 2736, 2964, 3192, 3420, 3648, and 3876 mm). All the attachments of the resistance strain gauges to the pile body were waxed to make them waterproof. Custom resistive soil-pressure sensors with an outside diameter of 20 mm and a thickness of 7 mm were attached to the pile surface along the pile length (114, 228, 342, 456, 570, 684, and 798 mm). The p-y curve and the ultimate soil resistance were studied through direct measurements of the soil resistance.

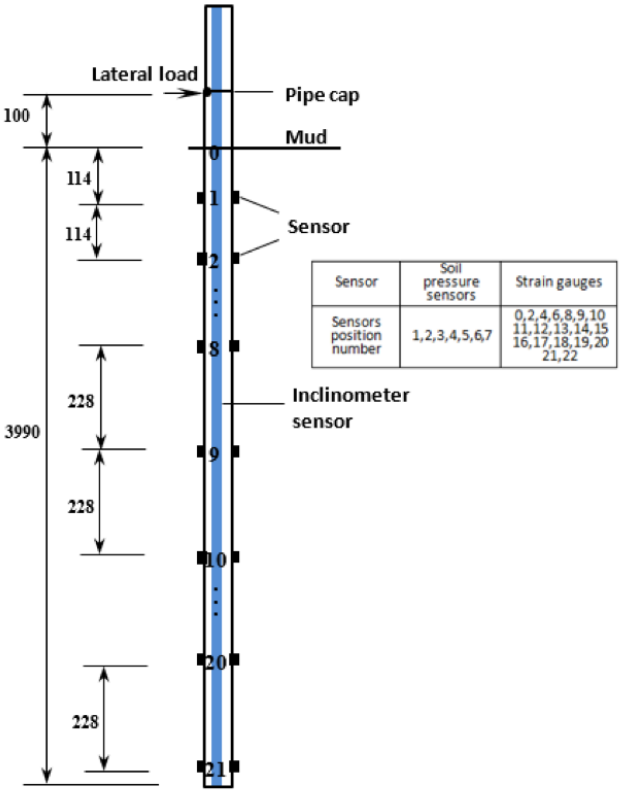

Figure 3. Pile instrumentation and the location of various sensors.

3 EXPERIMENTAL PROCESSES

3.1 Saturated clay preparation process

In the saturated-clay preparation process, uniform sand with a 0.5-mm particle size was first used to line the bottom of the soil pool to a depth of 500 mm. Next, drying clay was placed in the soil pool, and the soil was paved and compacted with each additional 20-mm-thick layer of clay. Saturated clay was prepared by saturating each layer of clay individually, with water slowly flowing in from the water inlet hole at the bottom of the soil pool. The water level was controlled to 200 mm above the soil surface in the soil pool, and a slow inflow rate was maintained. Each soil layer was kept standing for 4–5 h to ensure the uniform soil saturation. Following the completion of the clay saturation, the excess water on the clay surface was absorbed and the saturated clay was kept still for 5 days.

To characterize the soil, consolidated drained (CD) triaxial tests were performed. Then, 114-mm-diameter triaxial soil samples were tested at confining pressures of 25, 50, and 100 kPa from a depth of 75 mm. The strain rate was 0.01 mm/min. Figure 5 shows the measured deviator stress-axial strain and peak friction angle during the CD triaxial tests.

3.2 Soil drainage preparation process

Three drains at the bottom of the soil pool were opened following the completion of the first part of the test. The soil samples in the soil pool were weighed to calculate the water content at different depths every 2 h.

The permeability of the soil samples was high, as the water content over 7 days fell to 9.2%. We theorize that the clay moisture content is the optimal moisture content (Fig. 4). Figure 5 shows that the soil friction angle increased to 30.96° after the drainage of the soil samples (12.3%) and that the cohesion increased to 15.18 kPa (126.6%).

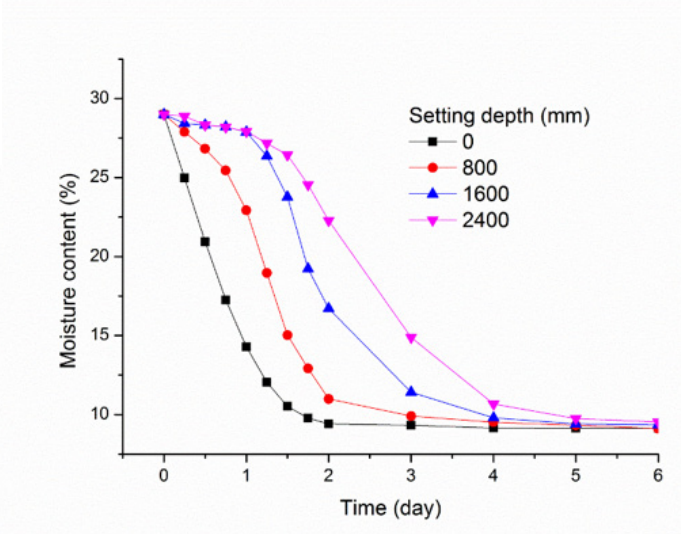

Figure 4. Drainage process at different soil moisture content depths.

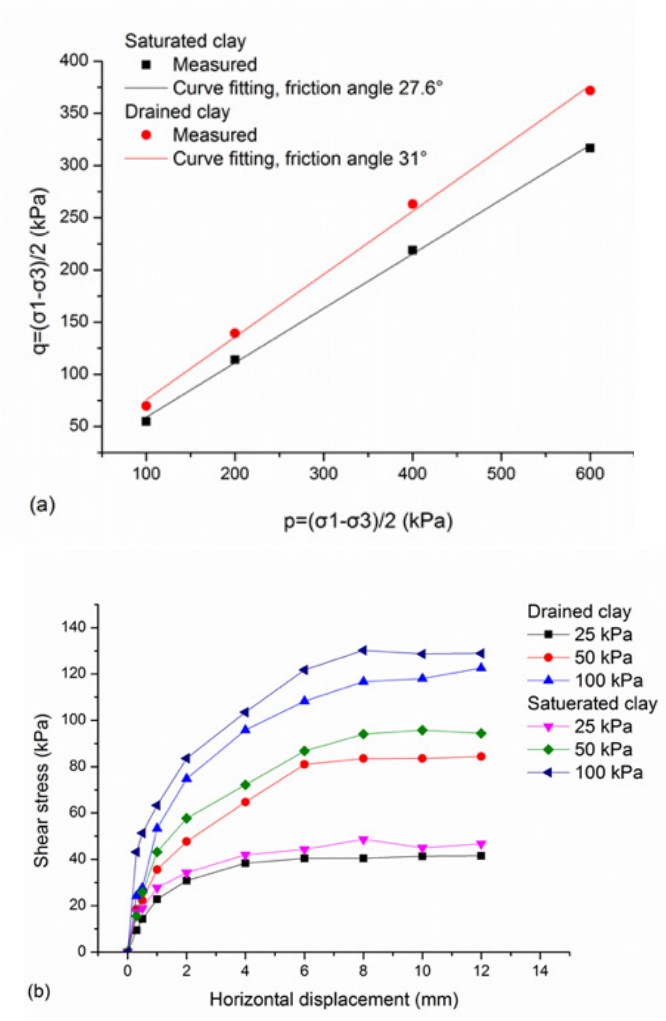

Figure 5. Properties of the soil used in the experiment: (a) results of CD triaxial tests performed on prepared soil samples and (b) p-q diagram of tested soil.

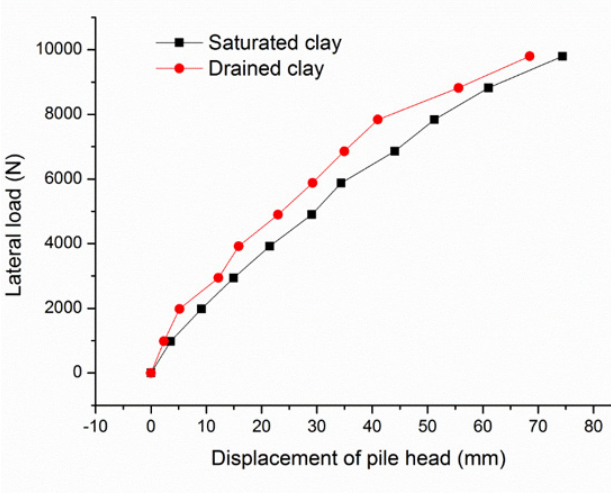

Figure 6. Lateral load-displacement curves at the pile head.

4 RESULTS

4.1 Load-displacement response at the pile head

Figure 6 shows the relationship between the measured lateral load and the pile-head displacement under saturated and unsaturated clay conditions. The figure shows that the lateral displacement of the pile head decreased with the increased *L/D*. Furthermore, as the load increased to 8330 N in the saturated clay, the displacement rate of the pile head increased; when the load increased to 9310 N after soil drainage, the pile-head displacement increased faster.

4.2 Strain along the pile length

The bending moments of the model pile can be calculated using Eq. (1) and the measurement results of the resistance strain gauges distributed along the pile length.

$$M_i = \frac{E \cdot \varepsilon \cdot I_i}{y} \qquad (1)$$

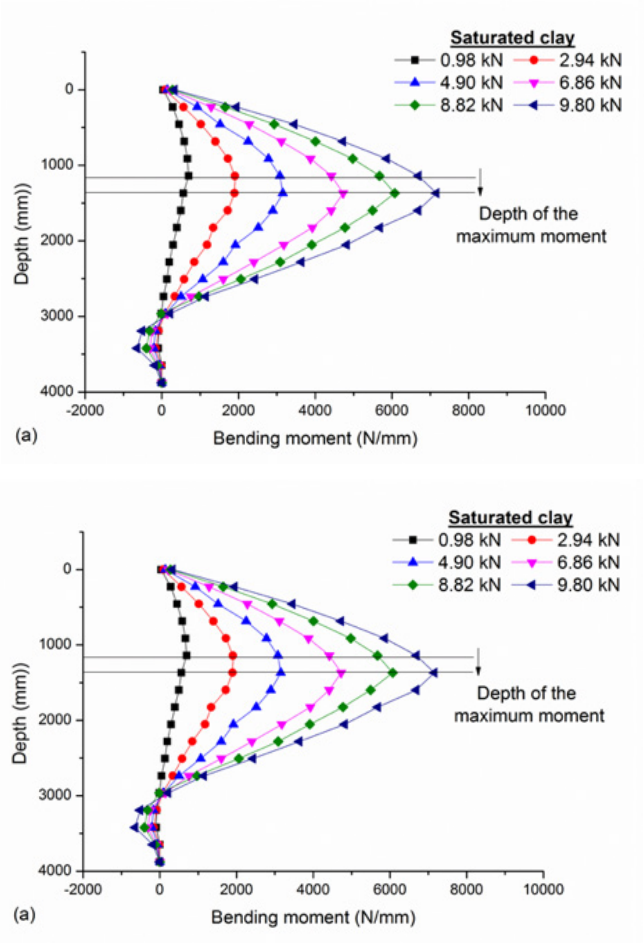

Figure 7. Bending-moment variation along the pile depth at different loading stages: (a) in saturated clay and (b) in drained clay.

where E is the elastic modulus of the model pile, Pa; ε is the strain value; I_i is the sectional moment of inertia, m4; and y is the resistance strain gauge distance from the neutral axis of the pile, m.

Figure 7 shows the lateral loading of the pile versus the bending moment in saturated and drained clays. The maximum peak moment of the pile was 7158 N·m (less than [M]) as the lateral load increased to 9.8 kN in the saturated soil. The depth of the maximum moment increased from 1140 to 1368 mm, and the zero point of the bending moment appeared 3 m below the surface of the mud.

In the drained soil samples, the maximum bending moment was 25% greater than that in the saturated soil. For the increased lateral load of 8.82 kN, the pile body appeared to undergo plastic deformation, and the depth of the maximum moment point was 1140 mm and did not increase further. As the lateral load was increased from 8.82 to 9.8 kN, the lateral displacement of the pile increased greatly. The same pile reached the plastic point earlier with a smaller load in the drained clay.

4.3 Pile-soil interaction along the pile length

In this study, the soil resistance of the piles was directly measured using soil-pressure sensors. The soil resistance can be calculated according to Eq. (2).

$$p = \mu\varepsilon \cdot K \qquad (2)$$

The p-y curve is a comprehensive index of the soil resistance around a pile. It is affected by the pile diameter, the stiffness, the cross-sectional shape, the size effect, and the pile end constraints. Soil resistance is normally calculated using an empirical formula; however, this result usually contains a large error. In fact, many studies have reported instances in which the p-y analysis results did not match the measured soil reaction profiles [13, 25].

Fig. 8 summarizes the measurements obtained using soil-pressure sensors installed along the pile length. Both figures show that the soil resistance increased as the applied lateral load increased.

Figure 9 shows the pile displacement during loading as measured using an inclinometer sensor and pile-head

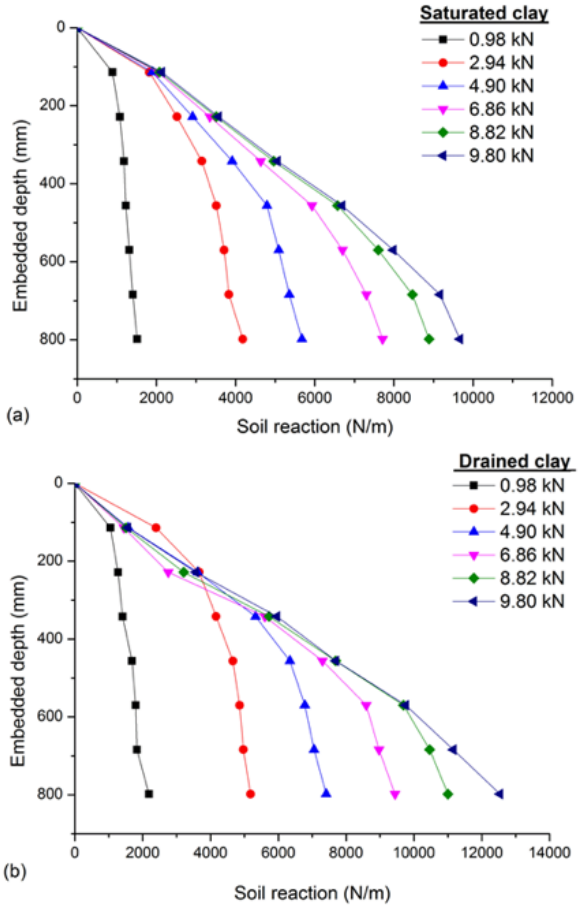

Figure 8. Measured soil reaction along the pile length at different loading stages: (a) in saturated clay and (b) in drained clay.

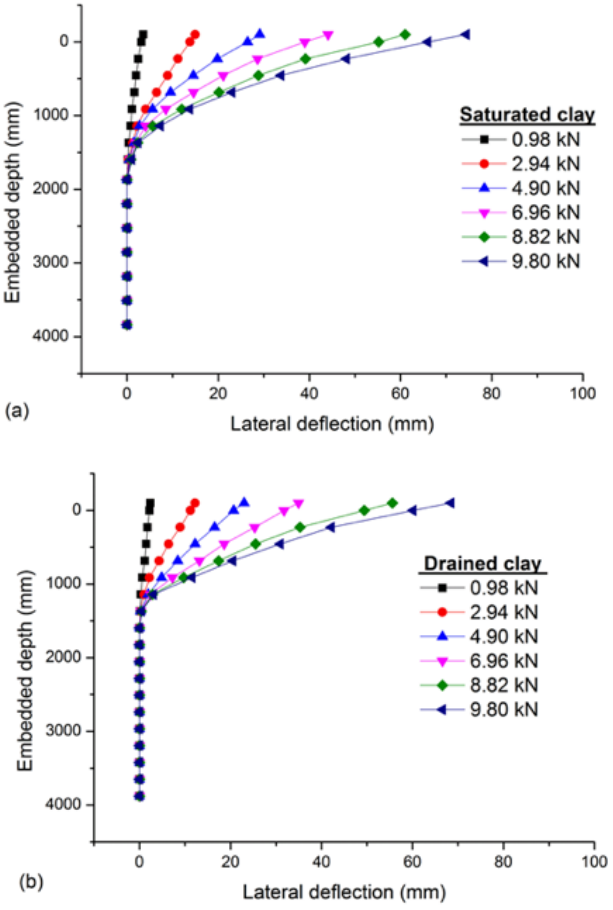

Figure 9. Lateral movement along the pile length at different loading stages: (a) saturated clay and (b) drained clay.

displacement sensor. In saturated soil, the loading point is located 100 mm above the mud line; the displacement at the top of the pile reaches 74.4 mm under a 9.8-kN lateral load, that at the mud surface is 66.0 mm, and a 10-mm bulge is seen on the mud surface with cracking. In drained clay, the lateral pile displacement is always lower than that in the saturated soil. The maximum displacement at the mud surface is 60.5 mm.

4.4 Soil-pile interaction force-displacement relationships (p-y curves)

The soil-pile interaction force per unit length (p) shown in Fig. 8 and the pile lateral displacement (y) shown in Fig. 9 were combined to produce directly measured p-y curves. Figure 10 shows directly measured p-y curves covering the pile length. The results show that the p-y curves increase with depth. There is no significant difference in the strength of shallow soils at depths of less than 228 mm. The soil resistance of the pile in drained clay is significantly reduced by a displacement of more than 15 mm with a 40% drop. This may be because of the shallow soil cracking caused by excessive pile displacement. However, in saturated clay, the soil resistance of the pile was not reduced. When the displacement reached 12 mm, the soil resistance became constant. In deeper soil layers, the soil resistance around the pile increased with the displacement, and the rate of increase was faster in drained clay, reflecting the increase in soil resistance after the clay drainage.

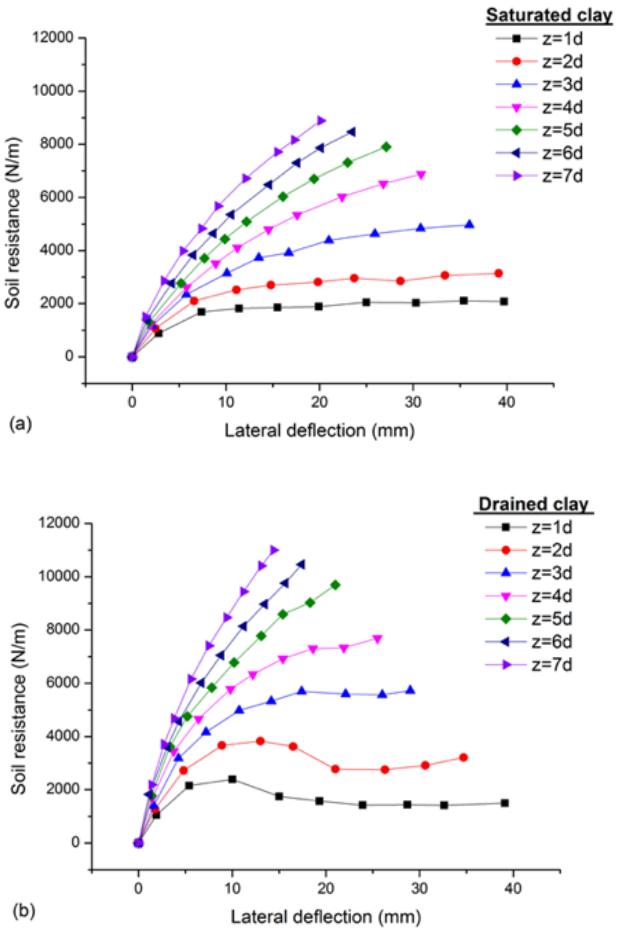

Figure 10. Relationship between the soil resistance and the displacement along the pile length at different depths: (a) pile in saturated clay; and (b) pile in drained clay.

5 DISCUSSION

Broms, Reese, Fleming, and Kim have established a model for the ultimate soil resistance around piles. In this study, the soil resistance was directly measured through a horizontal displacement experiment, and the soil resistance in drained clay was found to be increased compared with the initial value. The curve of the overlapping parts of the soil resistance at different loading stages is approximately a straight line. Figure 5 shows the measured soil friction angle (saturated soil friction angle φ_1=27.56°, drained clay friction angle φ_2=30.96°). According to Rankine's earth-pressure-calculation model, the ultimate resistance of the saturated and drained clay was expressed by Eqs. (3) and (4), respectively.

$$p_u = 4.76k_p \cdot \gamma \cdot z \qquad (3)$$

$$p'_u = 5.97k_p \cdot \gamma \cdot z \qquad (4)$$

Here, k_p is the passive earth-pressure coefficient (studies recommend a value of 3–9; [9, 14]); γ is the average effective weight of soil; and z is the embedded depth. The results reported in this study are ~24% lower than that

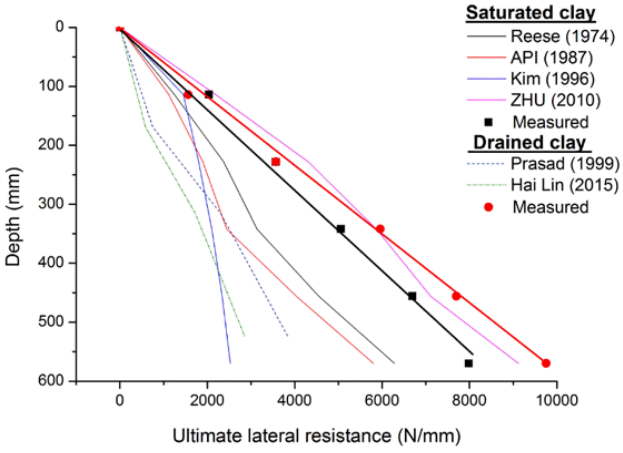

Figure 11. Comparison of the directly measured soil resistance at several depths and the p-y curves from other methods.

measured by Zhu [26] in saturated clays. The measured soil resistance in drained clay is up to 189% greater than that in unsaturated clay, as measured by Prasad and Chari [8]. The soil resistance in drained clay increased by 27% compared to that in saturated clay. At a depth of 114 mm the measured soil resistance deviated from the fitting curve; this is considered to be attributable to the bulging and cracks in the surface layer.

The directly measured p-y curves were compared with the p-y curves back-calculated from the measured strain profiles along the pile depth, which were obtained from the beam on elastic foundation theory. The measured bending moment of the pile was fitted by a sixth-order polynomial [26]. The soil resistance was calculated as $p(x) = d^2M / dx^2$. The soil resistance and pile lateral displacement at different loading stages were calculated as shown in Fig. 12. When compared with the back-calculated p-y curves at several depths along the pile length, the directly measured ultimate soil resistance per unit length showed smaller values than those back-calculated using the strain measurements. The difference was greater at depths closer to the maximum bending moment of the pile. The measured soil resistance at a depth of 798 mm was 37% smaller than the back-calculated one at a lateral load of 9.8 kN (Fig.12(a)). The difference in the soil resistance between the measured and back-calculated in drained clay was greater, up to 82%.

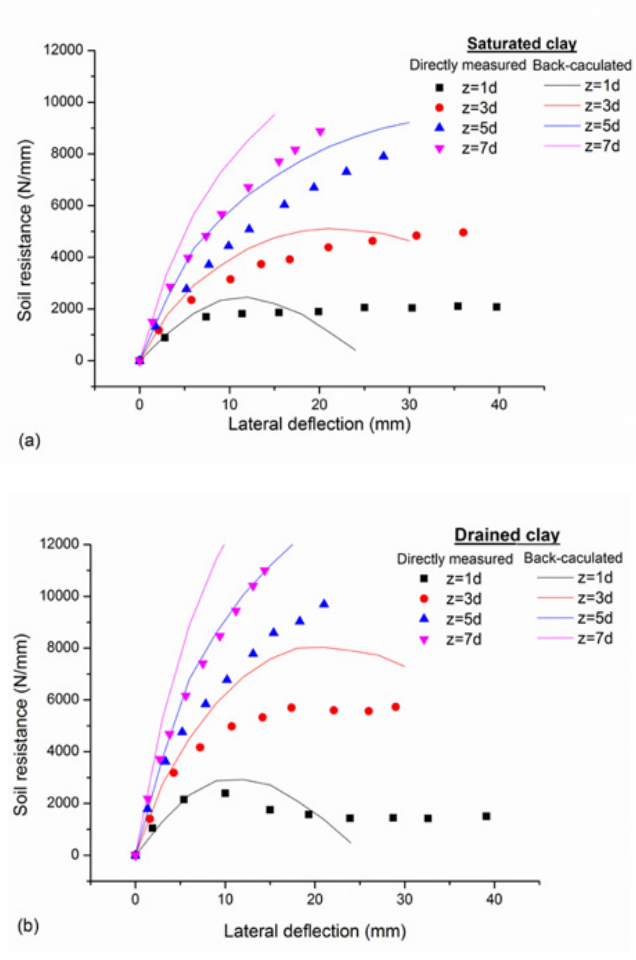

Figure 12. Comparison of the directly measured and the back-calculated p-y curves at several depths: (a) in saturated clay; and (b) in drained clay.

6 CONCLUSIONS

At present, the pile displacement, the bending moment, and the soil resistance around a pile are considered to be interrelated. Furthermore, several methods have been established for calculating the soil resistance around piles based on the displacement and bending moment. However, the measured results presented in this paper show that the results calculated by previous methods are not accurate, owing to the nonlinear characteristics of the soil.

The maximum bending moment depth of a pile first increases with the load and then remains constant, with the bottom of the pile fixed. When the pile body undergoes plastic deformation, the bending moment increases sharply; however, the soil resistance does not increase significantly, the pile still has a horizontal bearing capacity, and the level of deformation at this time increases significantly.

For bottom-fixed piles, the value of the maximum bending moment of the pile body in drained clay is greater for the same load, and the maximum bending moment depth is smaller. The lateral load-bearing capacity of the pile is greater than the initial value in saturated clay.

According to the test results, a model for the ultimate soil resistance of saturated and drained clays was established. The ultimate soil resistance of these two types of clay differed by 27%, and both increased linearly with depth. At a depth of 114 mm the measured soil resistance test deviated from the fitting curve. This is considered to be attributable to the bulging and cracks in the surface layer.

Although the bending moment of the pile is related to the soil resistance, there is a large error in building the polynomial anti-calculation soil resistance using the bending moment of the pile body. The back-calculated results of the soil resistance near the maximum bending moment depth deviate significantly from the measured values. This soil-resistance calculation method does not consider the fact that the distribution of the stiffness and the bending moment of the pile along the pile body is inconsistent with the distribution of the soil resistance along the depth.

REFERENCES

[1] Cheng, X., Jing, W., Yin, C., Li, C. 2018. Stability parameter analysis of a composite foundation of an oil storage tank in a loess area treated with compaction piles. Soils and Foundations, 58(2), 306-318. https://doi.org/10.1016/j.sandf.2018.02.004.

[2] Tananykhin, D., Tcvetkov, P., Kamoza, V. 2018. Wells. Journal of Physics: Conf. Series, 1072, 012022. https://doi.org/10.1088 / 1742-6596 / 1072/1/012022.

[3] Shagiakhmetov, A., Tananykhin, D., Terleev, A. 2018. Development of water-shutoff composition on the basis of carboxymethyl cellulose for fractured and fractured-porous oil and gas reservoirs. Acta Technica CSAV (Ceskoslovensk Akademie Ved), 63 (3), 475-480

[4] Brinch-Hansen, J. 1961. The ultimate resistance of rigid piles against transversal forces. Bulletin Representative No. 12, Danish Geotechnical Institute, Copenhagen, Denmark, 5-9.

[5] Reese, L.C., Cox, W.R., Koop, F.D. 1974. Analysis of laterally loaded piles in sand. Proceedings of the 6th Annual Offshore Technology Conference, Houston, Texas 2(OTC 2080), 473-485.

[6] Wesselink, B.D., Murff, J.D., Randolph, M.F., Nunez, I.L., Hyden, A.M. 1988. Analysis of centrifuge model test data from laterally loaded piles in calcareous sand. Engineering for calcareous sediments 1, 261-270.

[7] Yan, L., Byrne, P.M. 1992. Lateral pile response to monotonic pilehead loading. Canadian Geotechnical Journal 29, 955–970. https://doi.org/10.1139/t92-106.

[8] Prasad, Y.V., Chari, T.R. 1999. Lateral capacity of model rigid piles in cohesionless soils. Soils and Foundations 39(2), 21-29. https://doi.org/10.3208/sandf.39.2_21.

[9] Poulos, H.G., Davis, E.H. 1980. Pile foundation analysis and design. New York: John Wiley & Sons.

[10] Fleming, K., Weltman, A., Randolph, M., Elson, K. 2014. Piling engineering. CRC press.

[11] McClelland, B., Focht, J.A. 1958. Soil modulus for laterally loaded piles. Transactions, ASCE, 123, 1071-1074.

[12] Ashour, M., Norris, G. 2000. Modeling lateral soil-pile response based on soil-pile interaction. Geotechnique 126(5), 420–427. https://doi.org/10.1061/(ASCE)1090-0241.

[13] Matlock, H., Reese, L.C. 1960. Generalized solutions for laterally loaded piles. Soil Mech Found Division ASCE 86(5), 63-91.

[14] American Petroleum Institute. 1987. Recommended practice for planning, designing and constructing fixed offshore platforms. 17th ed. Washington D C: American Petroleum Institute, API-RP2A.

[15] O'Neill, M.W., Murchinson, J.M. 1983. An evaluation of p-y relationships in sand. Washington D C: American Petroleum Institute.

[16] Kondner, R.L. 1963. Hyperbolic stress-strain response: Cohesive soils. Journal of Soil Mechanics and Foundation Division 89(1), 115-144.

[17] King, G.J.W. 1994. The interpretation of data from tests on loaded piles. Centrifuge 94, 515-520.

[18] Duan, W.F., Liao, X.H., Jin, J.S., Wang, Y.Q. 2001. Numerical modeling of pile-soil interface and numerical analysis of single pile QS curve. Journal of Harbin University of Civil Engineering and Architecture 5, 007.

[19] Yinao, G.Z.S.K.S., Zhichuan, G., Kanhua, S. 2009. Analysis on lateral load-bearing capacity of conductor and surface casing for deepwater drilling. Acta Petrolei Sinica 2, 024.

[20] Kim, Y., Jeong, M.S., Lee, S. 2011. Wedge failure analysis of soil resistance on laterally loaded piles in clay. Geotech Geoenviron Eng 137(7), 678–694. https://doi.org/10.1061/(ASCE)GT.1943-5606.0000481.

[21] Yang, H.P., Zhang, R., Zheng, J.L. 2006. Variation of deformation and strength of expansive soil during cyclic wetting and drying under loading condition. Yantu Gongcheng Xuebao (Chinese Journal of Geotechnical Engineering) 28(11), 1936-1941.

[22] British Standards 1377. 1990. Parts 1 to 8 - Methods of Test for Soils Civil Engineering Purposes. British Standards Institution, London.

[23] Boominathan, A., Ayothiraman, R. 2007. Measurement and analysis of horizontal vibration response of pile foundations. Shock Vib 14(2), 89-106.

[24] Rao, S.N., Ramakrishna, V.G.S.T., Rao, M.B. 1998. Influence of rigidity on laterally loaded pile groups in marine clay. Journal of Geotechnical and Geoenvironmental Engineering 124(6), 542-549. https://doi.org/10.1061/(ASCE)1090-0241.

[25] Muthukkumaran, K. 2013. Effect of slope and loading direction on laterally loaded piles in cohesionless soil. International Journal of Geomechanics 14(1), 1-7. https://doi.org/10.1061/(ASCE)GM.1943-5622.0000293.

[26] Zhu, B., Zhu, R.Y., Luo, J., Chen, R., Kong, L. 2010. Model tests on characteristics of ocean and offshore elevated piles with large lateral deflection. Chinese Journal of Geotechnical Engineering 32(4), 521-530.